CRYSTAL GROWTH & DESIGN

Communication

pubs.acs.org/crystal

Creatine: Polymorphs Predicted and Found

Doris E. Braun,*[,†] Maria Orlova,[§] and Ulrich J. Griesser[†]

[†]Institute of Pharmacy and [§]Institute of Mineralogy and Petrography, University of Innsbruck, Innrain 52, 6020 Innsbruck, Austria

Supporting Information

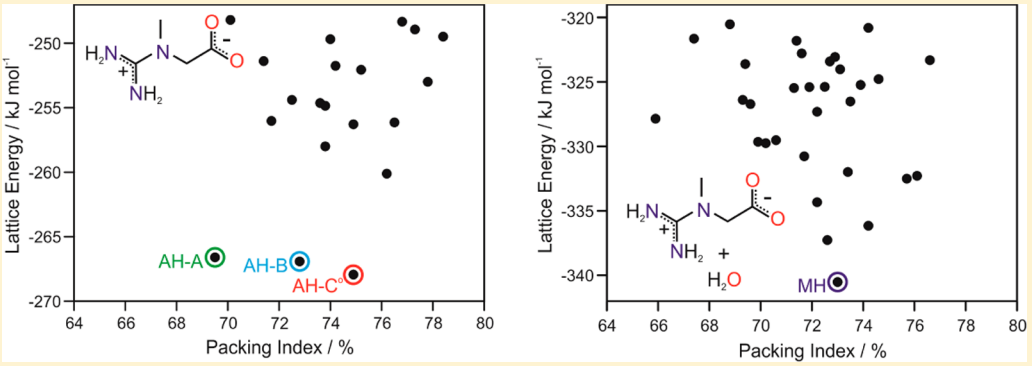

ABSTRACT: Hydrate and anhydrate crystal structure prediction (CSP) of creatine (CTN), a heavily used, poorly water-soluble, zwitterionic compound, has enabled the finding and characterization of its anhydrate polymorphs, including the thermodynamic room temperature form. Crystal structures of the novel forms were determined by combining laboratory powder X-ray diffraction data and ab initio generated structures. The computational method not only revealed all experimental forms but also predicted the correct stability order, which was experimentally confirmed by measurements of the heat of hydration.

Identifying and understanding the polymorphic behavior, including hydrate and solvate formation, is a key concern in the pharmaceutical and any other fine-chemical industries. This is because different solid forms can show variations in their physical properties, such as density, solubility, dissolution rate, hardness, melting point, mechanical strengths, chemical stability, and so forth, and thus influence manufacturing, long-term stability, and performance of the product.[1] Therefore, it is essential to search for practically relevant solid forms by varying the critical parameters that influence the occurrence of different forms, such as temperature, pressure, moisture, and the solvent of crystallization (including water activity). Moreover, it is important to examine the kinetics and thermodynamic stabilities of the crystal forms and to establish the most important transformation pathways. The knowledge of the crystal structures is often the key to a better understanding of the solid state phenomena.

CTN (*N*-(aminoiminomethyl)-*N*-methyl glycine) occurs naturally in vertebrates and is one of the most popular dietary supplements with estimated $2.7 billion in annual (2009) sales in the United States alone.[2a] The compound is widely consumed by athletes of many sports disciplines since it increases the formation of adenosine triphosphate (ATP) and improves the energy balance in muscles and also in the central nervous system.[2b] Though CTN was discovered already in 1832, clear evidence for the existence of only two solid state forms, an anhydrate (AH-**A**) and a monohydrate (**MH**), can be found in the literature until 2013.[3] The crystal structure of **MH** has been repeatedly determined either from powder[4] or single crystal data (CSD refcode[5] family: CREATH[6]). The AH-**A** structure was recently solved from powder X-ray diffraction (PXRD) data, supported by full ab initio predictions.[7] During the finalization of this manuscript, a report was published[8] which confirms that CTN is trimorphic and reports the structure of one new anhydrate and the formic acid monosolvate.

The insolubility of CTN in most solvents other than water, the fact that crystallization of CTN from aqueous solutions exclusively yields **MH**,[7] and the thermal decomposition to creatinine at a temperature above 230 °C[3a] drastically limit state of the art screens for alternative solid state forms.[9] This may be the main reason it took nearly 80 years to clearly confirm anhydrate polymorphism.[10,11] These limitations restricted our experimental options to slurry and dehydration studies, which were complemented with a computational search methodology (crystal structure prediction, CSP). Possible $Z' = 1$ crystal structures of CTN anhydrates and monohydrates were generated by searches for low energy local minima on the lattice energy surface,[12] and the lattice energies were evaluated accurately using dispersion corrected DFT calculations.[13] The structure of the known AH-**A** emerged as the third in energy on the anhydrate crystal energy landscape (Figure 1a). The findings of the anhydrate crystal energy landscape are in contrast to previously reported results,[7] which identified AH-**A**

Received: August 4, 2014
Revised: September 5, 2014
Published: September 8, 2014

   dx.doi.org/10.1021/cg501159c | *Cryst. Growth Des.* 2014, 14, 4895−4900

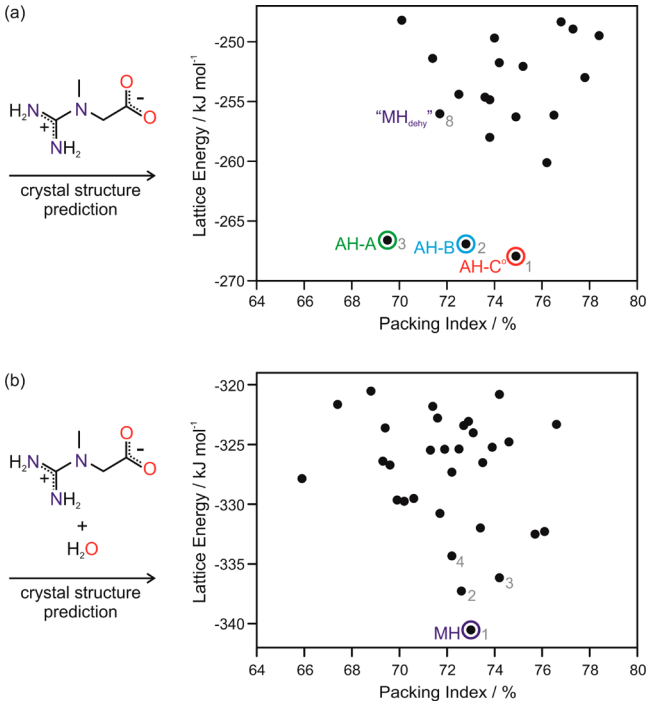

Figure 1. CTN crystal energy landscape for (a) anhydrates and (b) monohydrates. Each point denotes a computationally generated crystal structure. Experimental structures are encircled and selected structures labeled by their rank.

as the most stable structure, but no alternative polymorphs within 11.8 kJ mol^{-1} of AH-**A**. However, our CSP results indicated the existence of two additional anhydrates (Figure 1a).

The limited, but tailored, experimental solid form screen lead to two novel CTN anhydrates, AH-**B** and AH-**C°**, which were also found in an automated parallel crystallization/slurry screen published very recently.[8] AH-**B** (corresponding to form III in ref 8) is obtained as the dominating phase by fast dehydration of **MH** above the peritectic temperature (>126 °C) and AH-**C°** (corresponding to form I[8]) by slurring CTN in solvents (mixtures) at a water activity ≤0.26 at 25 ± 5 °C. These slurry experiments prove that AH-**C°** is the thermodynamically stable form at room temperature (denoted with "°").[14] Unfortunately, attempts to obtain single crystals of AH-**B** and AH-**C°** failed. However, the experimental PXRD patterns of the new forms indicate high crystallinity and were compared to the simulated PXRD patterns of the calculated low energy structures. The simulated patterns of the two lowest energy structures are in excellent agreement with the experimental patterns of the two novel anhydrates. Indexing[15] of the laboratory PXRD data resulted in comparable lattice parameters and space group agreement. This allowed us to determine the AH-**B** and AH-**C°** structures using PXRD data and the computationally generated structures as starting models for Rietveld refinements (Figure S14 of the Supporting Information).[16] The global minimum structure in Figure 1a corresponds to AH-**C°** (I[8]). The second-lowest energy structure corresponds to AH-**B** (III[8]).

The CTN molecule of AH-**B** ($P2_1/n$, $Z' = 1$)[17a] and AH-**C°** ($Pna2_1$, $Z' = 1$)[17b] adopts a conformation which is similar to those observed in AH-**A** and **MH** (see Section 8 of the Supporting Information). As the three CTN anhydrates differ solely in their packing arrangements, they may be classified as "packing polymorphs".[1c,18] The guanidinium C atom is

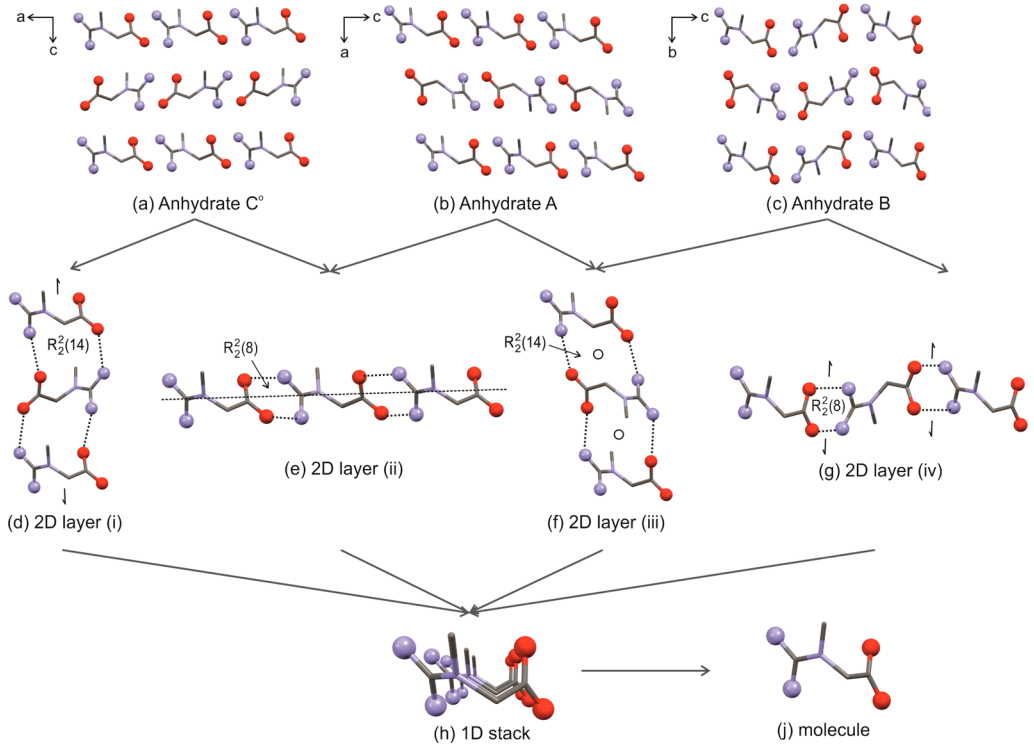

Figure 2. Structural comparisons of CTN anhydrates: (a–c) Packing diagrams of AH-**A**, AH-**B**, and AH-**C°**. (d–g) Layers (i–iv): layer (i) present in AH-**C°**, layer (ii) in AH-**C°** and AH-**A**, layer (iii) in AH-**A** and AH-**B**, and layer (iv) in AH-**B**. (h) Stacking motif of CTN molecules present in all structures. (j) CTN molecule. Selected symmetry operations and graph sets are indicated in (d–g). Hydrogen atoms are omitted for clarity.

dx.doi.org/10.1021/cg501159c | *Cryst. Growth Des.* 2014, 14, 4895–4900

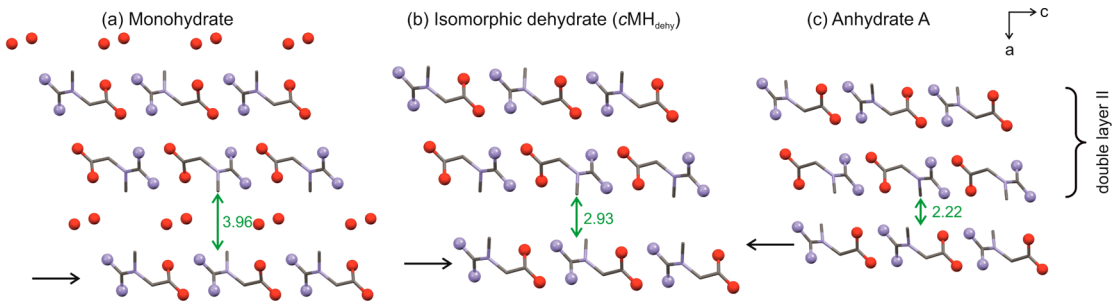

Figure 3. Packing comparison of (a) **MH**,[6d] (b) *c*MH$_{dehy}$, and (c) AH-**A**. Arrows and numbers in Å are interlayer distances (planes formed by $-CH_3$ carbons). Hydrogen atoms are omitted for clarity.

essentially coplanar with the three N atoms. Extensive hydrogen bonding of the amino groups results in nonplanar NH_2 groups, as confirmed by the PBE-D calculations. Each of the four N−H groups acts as an H-bond donor and each of the oxygen atoms as an H-bond acceptor for two N−H groups. The packing analysis of the three lowest energy structures (Figure 2a−c) resulted in four distinct types of layers with strongly N−H···O bound chain motifs (Figure 2d−f). Each of the chains involves either a $R_2^2(8)$ or $R_2^2(14)$ ring motif.[19] The $R_2^2(14)$ chains show a 2_1 symmetry in AH-**C**° and inversion symmetry in AH-**A** and AH-**B**, whereas the $R_2^2(8)$ ring chain is generated by *c*-glide operation in AH-**A** and AH-**C**° and 2_1 operation in AH-**B**. PIXEL calculations of pairwise energies[20] estimate the $R_2^2(14)$ motif as more stable than the $R_2^2(8)$ motif (−91.5 to −97 kJ mol^{-1} and −72 to −73.5 kJ mol^{-1}, respectively). All three anhydrates share the same 1D stacks of CTN molecules (Figure 2h); the polymorphic pair AH-**A**/AH-**B** shares layer (iii) (Figure 2f), and AH-**A**/AH-**C**° layer (ii) (Figure 2e).[21] Alternative stacking of the experimental layers, alternative chain motifs, or CTN conformations would be geometrically possible, but result in high energy structures as obtained in Figure 1a.

The **MH** structure was found to be the most stable structure in the corresponding crystal energy landscape (Figure 1b). The calculations show that three hypothetical structures (*c*MH2-*c*MH4) are thermodynamically plausible polymorphs when the effects of thermal motion are neglected, but structures *c*MH2 and *c*MH4 show sufficient structural similarity to the known monohydrate, making them unlikely to be observed (Section 5 of the Supporting Information). However, the structure of *c*MH3 is clearly different to **MH**, *c*MH2, and *c*MH4. The water molecules are part of a $R_2^2(8)$ dimer, and therefore it cannot be ruled out that this metastable form may be found one day. Its existence has not been established, neither in the present study nor in that of ref 8, and it remains a challenge to find suitable crystallization conditions and proof of the existence of this form.

The dehydration of **MH** below its peritectic temperature (T_{diss} = 125.8 ± 0.5 °C) leads exclusively to AH-**A**, which can be explained by the packing similarity of **MH** and AH-**A** (Figure 3). The water in the structure leads to a widening of the gap between every alternate layer (ii) construct from 2.22 to3.96 Å (planes formed by $-CH_3$ carbons) and causes a shift of adjacent double (ii) layers. The water molecules form four strong hydrogen bonds, two to water and two to CTN molecules. They are located in channels parallel to the *b*-axis and adsorption/desorption can occur while maintaining the structural layers of CTN molecules. The computationally generated hypothetical isomorphic dehydrate structure (*c*MH$_{dehy}$, Figure 3b) differs only slightly from AH-**A** in the stacking of double layer (ii) fragments, but by 11.6 kJ mol^{-1} in lattice energy due to long and less favorable N−H···O interlayer distances. The transformation from *c*MH$_{dehy}$ to MH-**A** is facile, making this intermediate unlikely to be experimentally accessible. This may explain why **MH** dehydrates to a distinct phase and not to an isomorphic desolvate (*c*MH$_{dey}$).[22]

A lower degree of similarity is observed between **MH**/AH-**B** and **MH**/AH-**C**°. **MH** and AH-**C**° share a single layer (ii) construct, and **MH** and AH-**B** layer (iii), but in the case of **MH**, they are interspersed with water. Transformation of **MH** to AH-**B** has been observed, but only at temperatures higher than T_{diss} of the **MH**, i.e., only by melting and recrystallization. Dehydration to AH-**C**° has not been observed yet.

Thermal analysis of the three anhydrates did not indicate any thermal event (e.g., a transformation) below 230 °C where the intramolecular cyclization to creatinine occurs. Furthermore, no transformation of the metastable AH-**A** and AH-**B** occurred during storage of the samples at a relative humidity (RH) < 30% at 25, 40, and 60 °C for 8 months. However, all three anhydrates transform to **MH** at elevated moisture conditions. The AH-**A** to **MH** transition occurs at RH > 35%, whereas AH-**B** and AH-**C**° transform at RH > 60%. The back-transformation of **MH** to AH-**A** occurs at RH < 20% RH (Figure 4a−d). Thus, only **MH** and AH-**B** and AH-**C**° are kinetically stable between 25% and 60% RH at 25 ± 5 °C, which is within the most common room climate conditions. Water activity (a_w) measurements in methanol/water mixtures (Figure S13 of the Supporting Information) revealed that the equilibrium between AH-**C**° and **MH** is at a_w = 0.27 (25 °C). Thus, anhydrous CTN only crystallizes from solvents exhibiting a_w < 0.27. At higher water activities **MH** will form.

Due to the thermal decomposition it was not possible to measure the heat of fusion of the three anhydrates with differential scanning calorimetry (DSC) and consequently to derive their thermodynamic stability order from these phase transition enthalpies. However, by measuring the heat of hydration of the anhydrous state to **MH**, $\Delta_{hy}H_{AH\text{-}MH}$ with isothermal calorimetry using the RH perfusion technique (Figure 4i−l, Table 1) we were able to experimentally determine the enthalpy differences between the three anhydrates to be −1.8 kJ mol^{-1} (AH-**A** → AH-**C**°) and −0.9 (AH-**B**→ AH-**C**°) kJ mol^{-1} (see Section 9 of the Supporting Information). Hydration to a specific hydrate is more energetic (exothermic) for a less stable form,[23] resulting in the stability order AH-**C**° (most stable) > AH-**B** > AH-**A** (least stable) for the CTN polymorphs. The calculated lattice energy differences corroborate this stability order and reinforce that the energy

dx.doi.org/10.1021/cg501159c | *Cryst. Growth Des.* 2014, 14, 4895−4900

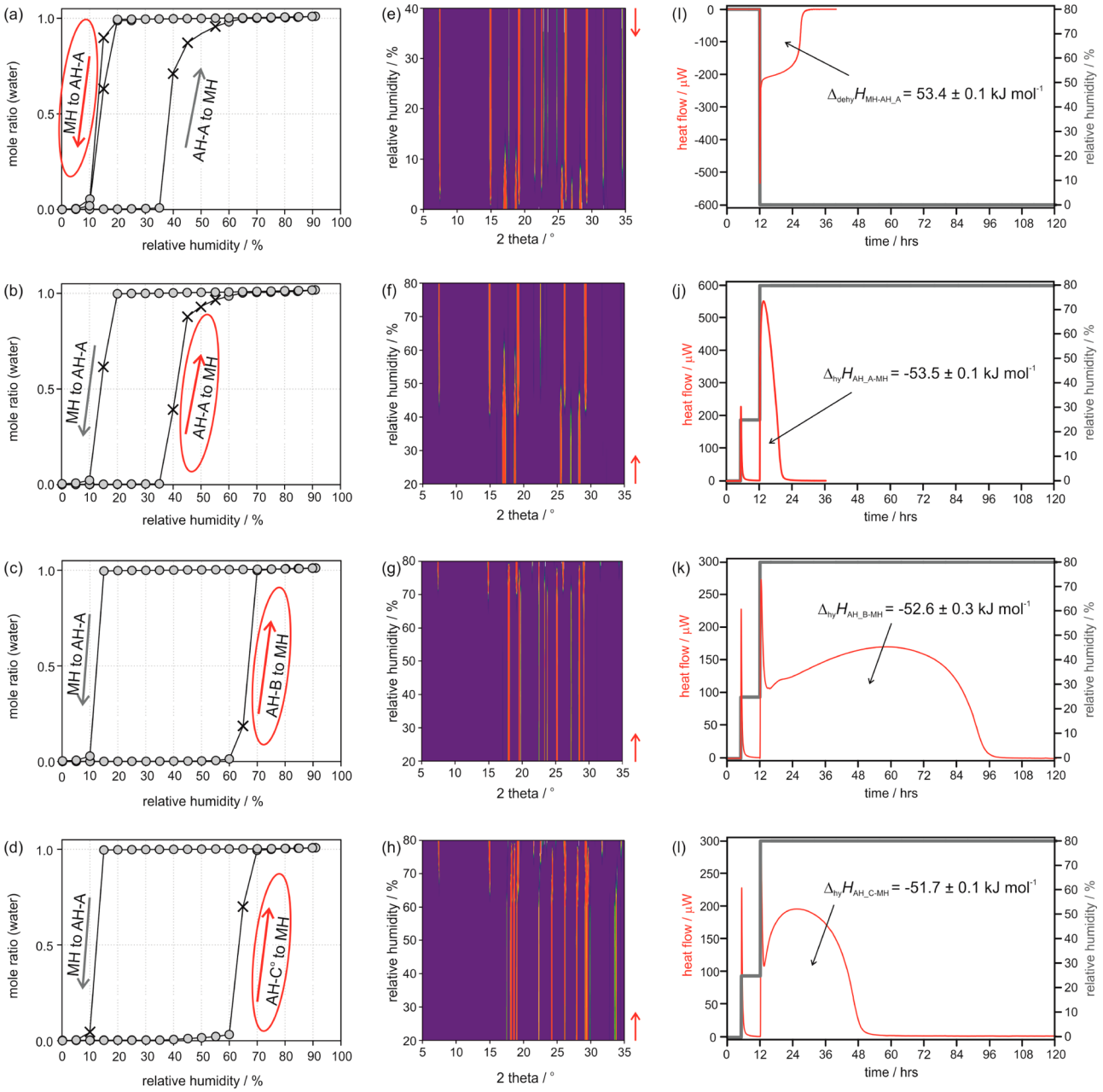

Figure 4. Moisture dependent hydration and dehydration reactions of CTN solid forms. (a–d) Gravimetric moisture sorption/desorption isotherms of CTN at 25 °C starting with (a) **MH**, (b) AH-**A**, (c) AH-**B**, and (d) AH-**C°**. The gray circles represent data points recorded at equilibrium conditions, and crosses mark measurements where equilibrium conditions have not been reached within the set time limit of 48 h. The arrows indicate the direction of the moisture changes, i.e., a sorption (increasing RH) or desorption cycle (decreasing RH). Encircled arrows correspond to the transformations measured with moisture dependent PXRD. Guinier plots: (e) **MH** to AH-**A**, (f) AH-**A** to **MH**, (g) AH-**B** to **MH**, and (h) AH-**C°** to **MH**. Red arrows mark the starting point. Isothermal calorimetry: (i) **MH** to AH-**A** (80% to 0% RH in one step), (j) AH-**A** to **MH**, (k) AH-**B** to **MH**, and (l) AH-**C°** to **MH** (all 0% to 25% RH in one step and 25% to 80% in one step).

differences between the polymorphs are fairly small, and finally confirm that hydrate formation is driven by greater potential energy.

Over 180 years after the discovery of CTN its thermodynamically stable polymorph at room temperature has been predicted and experimentally verified (independently by two groups[8]). The new anhydrates (AH-**B**, AH-**C°**) can be expected to show a higher solubility than the hydrate and it was found that they exhibit a higher hydration stability than the known anhydrous form (AH-**A**). These advantages could be beneficial for increasing the dissolution rate and may also lead toward a potential strategy to improve the limited bioavailability of CTN. However, the problem with compounds forming a very stable hydrate may be a fast transformation kinetics of the anhydrous form/s to this hydrate. If the hydrate formation is much faster than the dissolution process of the anhydrate, there is no benefit in using a more soluble anhydrate. For CTN anhydrates we observed a fast transformation to the hydrate in water, and we therefore suspect that the liberation from a tablet or capsule formulation is not considerably improved by using any of the anhydrous forms instead of the stable hydrate. A combined CSP/laboratory PXRD approach[7,24] allowed us to determine

dx.doi.org/10.1021/cg501159c | *Cryst. Growth Des.* 2014, 14, 4895–4900

Table 1. Thermodynamic Data and Lattice Energies Based on Periodic PBE-D Calculations for CTN Anhydrates and Monohydrate

Energy[a]	AH-A	AH-B	AH-C°	MH
		Isothermal Calorimetry, 25 °C		
$\Delta_{hy}H$/kJ mol^{-1}	−53.5 ± 0.1 (A→MH)	−52.6 ± 0.1 (B→MH)	−51.7 ± 0.1 (C°→MH)	–
$\Delta_{dehy}H$/kJ mol^{-1}	–	–	–	53.4 ± 0.1 (MH→A)
		Differential Scanning Calorimetry, 95 °C		
$\Delta_{dehy}H$/kJ mol^{-1}	–	–	–	51.1 ± 0.5 (MH→A)
		Lattice Energy Calculations, −273.15 °C		
E_{latt}/kJ mol^{-1}	−266.6	−266.9	−267.9	−340.5

[a] $\Delta_{hy}H$ − enthalpy of hydration, $\Delta_{dehy}H$ − enthalpy of dehydration, E_{latt} − lattice energy.

the crystal structures of the two new anhydrates. CSP complemented the experimental understanding of the system by giving valuable insight into the likely packing possibilities and energies by providing the set of low energy structures.[25] The measurement of the heat of hydration with RH-perfusion calorimetry has been proven a successful method for deriving energy differences between polymorphs. This approach is particularly valuable for a hydrate forming system for which no fusion data can be determined with DSC because of thermal decomposition. Hence, this combination of analytical and theoretical methods can help us overcome the problems encountered in solid form screening, processing, handling, and storage of (polymorphic) fine-chemicals.

■ ASSOCIATED CONTENT

Supporting Information

Computational and experimental details, conformational analysis, crystal structure prediction, PIXEL calculations, Hirshfeld plots, thermal analysis, moisture sorption/desorption studies, water activity measurements, infrared spectroscopy, structure determination, experimental and computed energy differences. This material is available free of charge via the Internet at http://pubs.acs.org.

■ AUTHOR INFORMATION

Corresponding Author

*Tel: +43(0)512 507 58653; E-mail: doris.braun@uibk.ac.at.

Author Contributions

The manuscript was written through contributions of all authors. All authors have given approval to the final version of the manuscript.

Notes

The authors declare no competing financial interest.

■ ACKNOWLEDGMENTS

The authors are grateful to Profs. C. C. Pantelides and C. S. Adjiman (Imperial College London) for the use of the CrystalPredictor and CrystalOptimizer programs and Prof. S.L. Price (University College London) for the use of the DMACRYS program and for helpful discussions. D.E.B. gratefully acknowledges funding by the Hertha Firnberg Program of the Austrian Science Fund (FWF, project T593-N19). This work was supported by the Austrian Ministry of Science BMWF as part of the UniInfrastrukturprogramm of the Focal Point Scientific Computing at the University of Innsbruck.

■ REFERENCES

(1) (a) Bernstein, J. *Polymorphism in Molecular Crystals*; Clarendon Press: Oxford, 2002. (b) Byrn, S. R.; Pfeiffer, R. R.; Stowell, J. G. *Solid-State Chemistry of Drugs*; 2nd ed.; SSCI, Inc.: West Lafayette, IN, 1999. (c) Brittain, H. G. *Polymorphism in Pharmaceutical Solids*; Informa Healthcare: New York, London, 2009; Vol. *192*. (d) Hilfiker, R. *Polymorphism in the Pharmaceutical Industry*; Wiley-VCH: Weinheim, 2006.

(2) (a) Jaeger, R.; Purpura, M.; Shao, A.; Inoue, T.; Kreider, R. B. *Amino Acids* **2011**, *40*, 1369−1383. (b) Wallimann, T.; Wyss, M.; Brdiczka, D.; Nicolay, K.; Eppenberger, H. M. *Biochem. J.* **1992**, *281*, 21−40.

(3) (a) Dash, A. K.; Mo, Y.; Pyne, A. *J. Pharm. Sci.* **2002**, *91*, 708−718. (b) Sakata, Y.; Shiraishi, S.; Otsuka, M. *Colloids Surf., B* **2004**, *39*, 187−193.

(4) (a) Wilson, C. C.; Shankland, N.; Florence, A. J.; Frampton, C. S. *Physica B* **1997**, *234*, 84−86. (b) Florence, A. J.; Shankland, N.; Shankland, K.; David, W. I. F.; Pidcock, E.; Xu, X.; Johnston, A.; Kennedy, A. R.; Cox, P. J.; Evans, J. S. O.; Steele, G.; Cosgrove, S. G.; Frampton, C. S. *J. Appl. Crystallogr.* **2005**, *38*, 249−259.

(5) Allen, F. H. *Acta Crystallogr., Sect. B* **2002**, *58*, 380−388.

(6) (a) Mendel, H.; Hodgkin, D. C. *Acta Crystallogr.* **1954**, *7*, 443−446. (b) Jensen, L. H. *Acta Crystallogr.* **1955**, *8*, 237−240. (c) Kato, Y.; Haimoto, Y.; Sakurai, K. *Bull. Chem. Soc. Jpn.* **1979**, *52*, 233−234. (d) Frampton, C. S.; Wilson, C. C.; Shankland, N.; Florence, A. J. *J. Chem. Soc. Faraday Trans.* **1997**, *93*, 1875−1879. (e) Arakali, A. V.; McCloskey, J.; Parthasarathy, R.; Alderfer, J. L.; Chheda, G. B.; Srikrishman, T. *Nucleosides Nucleotides* **1997**, *16*, 2193−2218. (f) Goswami, S.; Jana, S.; Hazra, A.; Fun, H. K.; Anjum, S.; Atta, u. R. *CrystEngComm* **2006**, *8*, 712−718.

(7) King, M. D.; Blanton, T. N.; Misture, S. T.; Korter, T. M. *Cryst. Growth Des.* **2011**, *11*, 5733−5740.

(8) Arlin, J.-B.; Bhardwaj, R. M.; Johnston, A.; Miller, G. J.; Bardin, J.; MacDougall, F.; Fernandes, P.; Shankland, K.; David, W. I. F.; Florence, A. J. *CrystEngComm* **2014**, *16*, 8197−8204.

(9) Llinas, A.; Goodman, J. M. *Drug Discover. Today* **2008**, *13*, 198−210.

(10) Evidence of dimorphism is given in ref 11.

(11) Huffman, H. M.; Ellis, E. L.; Fox, S. W.; Fox, S. W. *J. Am. Chem. Soc.* **1936**, *58*, 1728−33.

(12) (a) Karamertzanis, P. G.; Pantelides, C. C. *J. Comput. Chem.* **2005**, *26*, 304−324. (b) Karamertzanis, P. G.; Pantelides, C. C. *Mol. Phys.* **2007**, *105*, 273−291. (c) Pantelides, C. C.; Adjiman, C. S.; Kazantsev, A. V. In *Prediction and Calculation of Crystal Structures*; Atahan-Evrenk, Ş., Aspuru-Guzik, A., Eds.; Springer: Berlin, 2014; Vol. *345*, pp 25−58. (d) Kazantsev, A. V.; Karamertzanis, P. G.; Adjiman, C. S.; Pantelides, C. C. *J. Chem. Theory Comput.* **2011**, *7*, 1998−2016. (c) Price, S. L.; Leslie, M.; Welch, G. W. A.; Habgood, M.; Price, L. S.; Karamertzanis, P. G.; Day, G. M. *Phys. Chem. Chem. Phys.* **2010**, *12*, 8478−8490.

(13) (a) Clark, S. J.; Segall, M. D.; Pickard, C. J.; Hasnip, P. J.; Probert, M. J.; Refson, K.; Payne, M. C. *Z. Kristallogr.* **2005**, *220*, 567−570. (b) Perdew, J. P.; Burke, K.; Ernzerhof, M. *Phys. Rev. Lett.* **1996**, *77*, 3865−3868. (c) Vanderbilt, D. *Phys. Rev. B* **1990**, *41*, 7892−7895.

(d) Tkatchenko, A.; Scheffler, M. *Phys. Rev. Lett.* **2009**, *102*, 073005−1−073005/4. (4) Grimme, S. *J. Comput. Chem.* **2006**, *27*, 1787−1799.

(14) We named the forms according to the order of detection and did not adopt the Roman numbering scheme applied by ref 8 to avoid confusion with our established Kofler notation (Roman numerals in order of melting points).

(15) (a) Shankland, K.; David, W. I. F.; Sivia, D. S. *J. Mater. Chem.* **1997**, *7*, 569−572. (b) Markvardsen, A. J.; David, W. I. F.; Johnson, J. C.; Shankland, K. *Acta Crystallogr., Sect. A* **2001**, *57*, 47−54.

(16) Rodriguez-Carvajal, J. *Newsletter* **2001**, *26*, 12−19.

(17) (a) Crystal data of AH-**B**: $C_3H_9N_3O_2$, M_r = 131.13, monoclinic, space group $P2_1/n$, T = 290 K, sample formulation: powder, wavelength: 1.54056 Å, a = 5.4857(3) Å, b = 11.4417(4) Å, c = 9.9625(5) Å, β = 98.663(5) °, V = 618.16(5)Å^3, Z = 4, density = 1.409 g cm^{-3}, 2 θ range for data collection: 5−111°, background treatment: set of consecutive points with refineable intensities, No. of measured reflections: 976, Refinement method: Rietveld with soft constraints, χ^2 = 2.12, R_{wp} = 4.53%, R_{exp} = 3.15%, R_p = 3.28%, CCDC no.: 1016214. (b) Crystal data of AH-**C°**: $C_3H_9N_3O_2$, M_r = 131.13, orthorhombic, space group $Pna2_1$, T = 290 K, sample formulation: powder, wavelength: 1.54056 Å, a = 11.9504(3) Å, b = 5.3453(2) Å, c = 9.5314 (3) Å, V = 608.86(3)Å^3, Z = 4, density = 1.431 g cm^{-3}, 2 θ range for data collection: 5−116°, background treatment: set of consecutive points with refineable intensities, No. of measured reflections: 569, Refinement method: renstrained Rietveld, χ^2 = 2.01, R_{wp} = 4.40%, R_{exp} = 3.11%, R_p = 3.32, CCDC no.: 1016215.

(18) Braun, D. E.; Gelbrich, T.; Kahlenberg, V.; Laus, G.; Wieser, J.; Griesser, U. J. *New J. Chem.* **2008**, *32*, 1677−1685.

(19) (a) Etter, M. C. *Acc. Chem. Res.* **1990**, *23*, 120−126. (b) Bernstein, J.; Etter, M. C.; Leiserowitz, L. In *Structure Correlation*; Burgi, H. B., Dunitz, J. D., Eds.; Wiley, 1994; pp 431−507.

(20) (a) Gavezzotti, A. *J. Phys. Chem. B* **2002**, *106*, 4145−4154. (b) Gavezzotti, A. *J. Phys. Chem. B* **2003**, *107*, 2344−2353.

(21) (a) Gelbrich, T.; Hursthouse, M. B. *CrystEngComm* **2006**, *8*, 448−460. (b) Gelbrich, T.; Threlfall, T. L.; Hursthouse, M. B. *CrystEngComm* **2012**, *14*, 5454−5464.

(22) Griesser, U. J. In *Polymorphism: In the Pharmaceutical Industry*, Hilfiker, R., Ed.; Wiley-VCH: Germany, 2006; pp 211−233.

(23) Lehto, V. P.; Laine, E. *Pharm. Res.* **2000**, *17*, 701−706.

(24) (a) Braun, D. E.; Bhardwaj, R. M.; Florence, A. J.; Tocher, D. A.; Price, S. L. *Cryst. Growth Des.* **2013**, *13*, 19−23. (b) Wu, H.; Habgood, M.; Parker, J. E.; Reeves-McLaren, N.; Cockcroft, J. K.; Vickers, M.; West, A. R.; Jones, A. G. *CrystEngComm* **2013**, *15*, 1853−1859. (c) Braun, D. E.; McMahon, J. A.; Koztecki, L. H.; Price, S. L.; Reutzel-Edens, S. M. *Cryst. Growth Des.* **2014**, *14*, 2056−2072.

(25) (a) Price, S. L. *Acta Crystallogr., Sect. B* **2013**, *69*, 313−328. (b) Price, S. L. *Chem. Soc. Rev.* **2014**. (c) Eddleston, M. D.; Hejczyk, K. E.; Bithell, E. G.; Day, G. M.; Jones, W. *Chem.—Eur. J.* **2013**, *19*, 7883−7888. (d) Kendrick, J.; Stephenson, G. A.; Neumann, M. A.; Leusen, F. J. *Cryst. Growth Des.* **2013**, *13*, 581−589. (e) Braun, D. E.; Tocher, D. A.; Price, S. L.; Griesser, U. J. *J. Phys. Chem. B* **2012**, *116*, 3961−3972. (f) Braun, D. E.; Bhardwaj, R. M.; Arlin, J. B.; Florence, A. J.; Kahlenberg, V.; Griesser, U. J.; Tocher, D. A.; Price, S. L. *Cryst. Growth Des.* **2013**, *13*, 4071−4083.